

The Fragile State of Industrial Agriculture: Estimating Crop Yield Reductions in a Global Catastrophic Infrastructure Loss Scenario

Jessica Moersdorf^{1,2}, Morgan Rivers², David Denkenberger^{2,3}, Lutz Breuer^{1,4}, Florian Ulrich Jehn^{1,2}

¹Institute for Landscape Ecology and Resources Management (ILR), Research Centre for BioSystems, Land Use and Nutrition (iFZ), Justus Liebig University Giessen, Heinrich-Buff-Ring 26, 35390 Giessen, Germany

²Alliance to Feed the Earth in Disasters (ALLFED), USA

³Department of Mechanical Engineering, University of Canterbury, Christchurch, Canterbury, New Zealand

⁴Centre for International Development and Environmental Research (ZEU), Justus Liebig University Giessen, Senckenbergstraße 3, 35392 Giessen, Germany

Corresponding author: Florian Ulrich Jehn (florian.u.jehn@umwelt.uni-giessen.de)

Key Points:

- Industrial agriculture is heavily dependent on external inputs such as machinery, fertilizers, and pesticides.
- A global catastrophe that inhibits the usage of electricity could reduce agricultural inputs, which would likely have a significant impact on crop yields.
- Regions with high levels of industrialization in agriculture, such as Europe, North and South America, India, China, and Indonesia, are projected to face major yield reductions.

Code Availability

Code can be found at <https://github.com/allfed/LosingIndustryCropYields> (Moersdorf et al., 2023)

Data Availability

Data is available as specified in Table 1.

Competing Interests

We have no competing interests to declare.

Abstract

Modern civilization is highly dependent on industrial agriculture. Industrial agriculture in turn has become an increasingly complex and globally interconnected system whose historically unprecedented yield relies strongly on external energy inputs in the shape of machinery, fertilizers, and pesticides. This leaves the system vulnerable to disruptions of industrial production and international trade. Several events have the potential to damage electrical infrastructure on a global scale, including electromagnetic pulses caused by solar storms or the detonation of nuclear warheads in the upper atmosphere, a pandemic leading to a significant reluctance to attend their workplaces, as well as a globally coordinated cyber-attack. The COVID-19 pandemic has highlighted the importance of crisis preparation and the establishment of more resilient systems. To improve preparation for high-stake risk scenarios their impact especially on critical supply systems must be better understood. To advance understanding of the implications for the global food system, this work aims to estimate the effect a global curtailment of industrial production could have on crop yields of the major staple crops: corn, rice, soybean, and wheat. We use a generalized linear model to estimate the loss in crop yield based on temperature, moisture, soil characteristics, nitrogen and pesticide application rates, the fraction of irrigated area and mechanization. The model predicts crop yields in two phases following a global catastrophe which inhibits the usage of any electric services. Phase 1 reflects conditions in the year immediately after the catastrophe, assuming the availability of fertilizer, pesticides, and fuel stocks. However, those stocks would be subject to rationed use in the first year. In phase 2, all stocks are used up and artificial fertilizer, pesticides and fuel are not available anymore. The predictions show a reduction in yield of 15 to 37 % in phase 1 and between 35 to 48 % in phase 2 depending on the crop. Soybean is least affected while wheat, rice and corn decline roughly by the same amount. Overall Europe, North and South America and large parts of India, China and Indonesia are projected to face major yield reductions of up to 95% while most African countries are scarcely affected. The findings clearly indicate hotspot regions which align with the level of industrialization of agriculture and highlight the need for preparation.

Plain Language Summary

Industrial farming plays a critical role in modern society but relies heavily on energy inputs. This complex and connected system is vulnerable to damage to industrial production and global trade. Potential events, such as solar storms, nuclear detonations, or cyber-attacks, can damage the global electrical infrastructure. The COVID-19 pandemic has shown the importance of preparedness and resilient systems. To understand the impact of high-risk events on critical supply systems, this study examines the effects on crop yields of corn, rice, soybean, and wheat. Using a model, the study estimates that a global catastrophic infrastructure loss would lead to yield reductions of 15% to 37% in Phase 1 (assuming the existence of remaining input stocks) and 35% to 48% in Phase 2 (when stocks are depleted). Europe, North and South America, as well as parts of India, China, and Indonesia, would experience major yield reductions, while most African countries would be less affected. These findings highlight regions at risk due to the level of industrialization in agriculture and emphasize the need for preparation. Understanding the consequences of global disruptions is crucial for building resilience in our food systems.

1 Introduction

The development of agriculture was a major turning point in human history. By offering a stable food source throughout the year, agriculture facilitated the emergence of complex societies all around the globe (Smil, 2017). Agricultural practices developed simultaneously in multiple different cultures, but yields were low and crop production labor intensive: despite its merits, food production in agricultural societies still required the involvement of most of the population to feed everyone. It was not until the rise of modern technology which allowed the harnessing of energy from fossil fuels and its introduction into agriculture in the shape of machinery, artificial fertilizer, and pesticides during the twentieth century that human populations could grow into the billions. This stark increase was supported by an expansion of cropland by 40% (Cao et al., 2021) and by substantially decreasing the number of human work hours required to produce one ton of grain from 30h/t in 1800 to just 90 min/t in 2000 (Smil, 2017).

But the rapid agricultural and societal development has severe consequences, like devastating environmental effects (Steffen et al., 2015), challenges related to climate change (Wiebe et al., 2015), and the decreasing rates of yield increase (van Ittersum et al., 2013), that also interact with each other. One crucial aspect, however, has been underreported in the literature: The advances of modern technology in agriculture have also resulted in a strong dependence of food security on global trade and industrial infrastructure (Neff et al., 2011). This makes the system vulnerable to events in which industrial infrastructure is disrupted. Especially on a global scale, the impact can be disastrous. The COVID-19 pandemic has demonstrated that events deemed highly unlikely can still occur at any given time and has exposed the lack of preparedness in most countries (Liu et al., 2020).

Research in recent years has highlighted the importance of one critical system for human survival in case of global catastrophic risk (Bostrom & Cirkovic, 2008): the food production system (Avin et al., 2018; Baum et al., 2015). Avin et al. (2018) argue that it is affected by most global catastrophic risks and that it constitutes the mechanism by which many global catastrophic risks endanger humanity's survival, namely by compromising agricultural production to the point of mass starvation. Society is highly dependent on modern agriculture as it enables most of the population to occupy themselves with tasks beyond food production (Coates, 2009; Diamond, 2011). This remarkable surplus in food and energy production can only be maintained through high external inputs into the production system in the form of machinery, fertilizers, and pesticides (Alston & Pardey, 2014). The importance of external inputs differs notably by country as there is no one uniform agricultural production system and stark differences between countries and world regions remain. However, the global food production system can be identified as a fragile system (Manheim, 2020) which is prone to systemic cascading failures (Goldin & Vogel, 2010; Helbing, 2013). Hence, even countries with lower industrial dependence are part of the increasingly connected global system and thus, likely to be subjected to the ripple effects of cascading failures. These properties, high industrial dependence and global interconnectedness, have only developed within the last 100 years but have quickly disseminated and profoundly and lastingly changed society.

This work examines the anticipated change in agricultural yield in a catastrophic infrastructure loss scenario. The underlying premise of all possible causes for catastrophic infrastructure loss is a global-scale disruption of the electrical grid. Given the widespread dependence of global industry and society on electricity, a global electrical failure would

essentially bring most industries and machinery to a standstill. The four main potential causes for global catastrophic infrastructure loss include:

- High Altitude Electromagnetic Pulses (HEMP) result from nuclear detonations high in the atmosphere. They cause no immediate harm to humans but can almost instantly damage electronics. Detonating a nuclear warhead emits gamma rays that interact with the atmosphere, creating an intense electromagnetic pulse (EMP) spreading at light speed. The disruptive EMP causes electronics to suffer overvoltage, like a more powerful lightning strike (Wilson, 2008). The affected area depends on the detonation's power and altitude; Wilson (2008) suggests one detonation could affect the entire contiguous United States. Multiple warheads during a nuclear conflict could lead to a global catastrophe. Recovery would likely be difficult, as critical infrastructure like large power transformers are often highly customized and currently need 12-24 months for production (Cooper & Sovacool, 2011).
- A similar risk is posed by solar storms. Solar activity during storms can present itself in the form of solar flares, coronal mass ejections or both. Solar flares are bursts of x- and gamma rays and extreme ultraviolet radiation which can disrupt communication technology (Baum, 2023; Cliver et al., 2022). Weiss and Weiss (2019), however, rate it as a minor risk and rather emphasize the effect of coronal mass ejections on the American power grid. This type of solar activity releases supercharged plasma particles towards earth, creating a geomagnetic storm which acts like a natural EMP towards the electrical grid with potentially devastating consequences (Baum, 2023; Cooper & Sovacool, 2011; Talib & Mogotlhwane, 2011). Like HEMPs, coronal mass ejections can permanently damage large power transformers and thus potentially cause power outages lasting for years (Cooper & Sovacool, 2011).
- Globally coordinated cyber-attacks on many electrical grids or critical industrial infrastructure pose a threat on a global catastrophic scale. Among the various systems under attack, power generation is a prime target for these cyber-attacks (Ogie, 2017). Until now, such attacks have been relatively limited in scope, but there is concern that more advanced and motivated actors could cause significant damage and disruption to these essential systems on a larger scale.
- An extreme pandemic could cause people to be too fearful to report to work in critical industries, resulting in a collapse of the power grid and other infrastructure, as maintenance ceases (Denkenberger et al., 2021).

Apart from the specific scenarios described above, the fragile world hypothesis introduced by Manheim (2020) can also induce or aggravate a loss of industry scenario. Manheim (2020) states that the world has become increasingly more complex, interconnected and most importantly less resilient. The economy's incentives to minimize redundancy have led to systems becoming progressively more fragile and hence more vulnerable to disruptions. Moreover, fragile systems can significantly worsen the impact of one of the loss of industry scenarios by leading to faster and more severe systems' collapses during a catastrophe.

All this highlights that it is important to increase the stability of our food system. Resilience efforts for the food production system vary depending on the type of catastrophe. For sun-blocking scenarios like a supervolcanic eruption this includes the exploration and preparation of resilient foods such as single cell protein from natural gas (García Martínez et al., 2022), hydrogen (García Martínez et al., 2021), sugar from wood (Throup et al., 2022),

greenhouses (Alvarado et al., 2020) or seaweed (Jehn et al., 2023). Most of these sources, however, depend on industrial infrastructure in one way or another. Therefore, for global catastrophic infrastructure loss scenarios, the adaptation of classical agricultural practices is the main method to ensure provision. Earlier work has suggested that this could revert agricultural yield to preindustrial levels (Cole et al., 2016).

To better gauge the impact the inhibition of industrial infrastructure can have, this work seeks to present a first spatial estimate of the expected changes in agricultural yield in the case of a global catastrophic infrastructure loss. Based on a multiple regression model using spatial predictors, we project yields for a worst-case scenario to understand the effects of a disturbance of industrial infrastructure on modern agriculture.

2 Materials and Methods

2.1 Selection of model crops and influencing factors

We modeled yields of wheat, corn, rice and soybean. They were chosen due to their status as staple crops, which was determined by considering their yearly production quantity and harvested area as reported by FAOSTAT. Globally, wheat and rice are the major food staples. Corn and soybean production is primarily used as livestock and aquaculture feed. Therefore, both crops have an enormous potential in a global catastrophic infrastructure loss scenario because their production can be diverted to human consumption. Apart from the potential use shift, soybean is the only legume and the only oil crop considered in the analysis. Legumes could play a crucial role for buffering nitrogen availability in the soil in absence of industrial fertilizers and soybean is the globally most widely produced legume.

Crop yield is influenced by a variety of factors (Neumann et al., 2010; Rabbinge, 1993; van Ittersum et al., 2013). The yield influencing factors used as model inputs for the analysis were chosen based on two selection criteria:

1. We identified key factors that played a pivotal role for progress in agriculture from preindustrial to modern times. Consequently, we selected mechanization, fertilizer, irrigation, and pesticides, in conjunction with enhanced crop varieties.(Alston & Pardey, 2014; Evenson & Gollin, 2003; Smil, 2017).
2. All factors with inadequate data availability that fell short of the spatial data resolution of five arcminutes at a global scale were excluded. Therefore, the improved varieties had to be excluded in the second step due to insufficient data availability. This exclusion of relevant variables likely leads to an underestimation of yield loss, but cannot be avoided as no global, high quality data is available.

The availability of the factors listed above is directly dependent on the management decisions of the farmer. However, there are also influential elements like climatic conditions which cannot be managed. To control for their impact on crop yield, three climatic variables representing thermal, moisture and soil conditions are considered in the analysis.

2.2 Spatial data

Global spatial datasets were sourced for each factor as well as for yields under current conditions. Datasets were selected at five arcminutes resolution when available or downsampled

to this resolution (Table 1; additional information can be found in Description_input_data.pdf in the repository of this paper (Moersdorf et al., 2023)).

Table 1: Datasets used for calibrating the generalized linear model and simulating loss of industry scenario conditions.

Dataset	Definition	Spatial resolution	Year	Source	Available online
SPAM	yield (kg/ha), harvested area (ha/cell)	5 arcmin	2010	(Yu et al., 2020)	https://doi.org/10.7910/DVN/PRFF8V
GAEZ v4 AEZ Factors	thermal regime class, moisture regime class, soil/terrain related class	5 arcmin, 5 arcmin, 30 arcsec	2010	(Fischer, 2021)	https://gaez.fao.org/pages/data-viewer
PEST-CHEMGRIDS	application rate (kg/ha) of 20 active ingredients for 10 dominant crops and 4 aggregated crop classes	5 arcmin	2015	(Maggi et al., 2019)	https://doi.org/10.7927/wcq9-pv30
Global Map of Irrigation Areas - Version 5	area equipped for irrigation (% of total area)	5 arcmin	2005	(Siebert et al., 2013)	https://data.apps.fao.org/map/catalog/srv/api/records/f79213a0-88fd-11da-a88f-000d939bc5d8
AQUASTAT - FAO's Global Information System on Water and Agriculture	Area (1000 hectares) equipped for: Irrigation (Equipped Lowland Areas, Spate Irrigation, Total) Full control irrigation (Surface, Sprinkler, Localized, Total, Actually Irrigated) Power irrigation	Country level	Around mid 2010s	(FAO, 2019)	http://fao.org/aquastat/statistics/query/index.html?lang=en
Gridded nitrogen and phosphorus fertilizer use	N and P application rate (g/m ²)	0.5°degree	1900-2013	(Lu & Tian, 2016)	https://doi.pangaea.de/10.1594/PANGAEA.863323
Global gridded dataset of manure nitrogen production and application	N manure application (kg/km ²)	5 arcmin	1860-2014	(Zhang et al., 2017)	https://doi.pangaea.de/10.1594/PANGAEA.871980
A global gridded data set on tillage (V. 1.1)	6 tillage systems (dominant system/cell)	5 arcmin	around 2005	(Porwollik et al., 2019)	https://doi.org/10.5880/PIK.2019.009

The N manure and N fertilizer application rate datasets from Table 1 were summed up into a combined variable N total, as the analysis is only concerned with the effect reduced N input has on yield and not with the effect of N input from different sources. Moreover, it was taken as a measure to reduce the number of variables and possible multicollinearity between them. Nitrogen management could not be considered due to a lack of suitable, global data. The

data pre-processing described in the next section was done before this merge, to be able to detect outliers.

Mechanization is the only selected factor which requires the use of a proxy as no spatially explicit data on the degree of mechanization in agriculture is available. We used the “global gridded data set on tillage (V. 1.1.)” (Porwollik et al., 2019) as a surrogate to determine if an area is farmed with motorized agricultural machinery or based on human and animal draft power. A large factor for the classification of tillage systems is the involvement of heavy machinery as it facilitates plowing soils in greater depth. Hence, it is possible to use the tillage systems as a proxy to determine which systems rely on machinery for tilling and which do not. We assume other farm activities such as sowing and harvesting are also carried out with machinery if tilling is mechanized. Therefore, the tillage systems are reclassified into either 0 = non-mechanized or 1 = mechanized. Conservation agriculture is classified as mechanized even though tillage is reduced to almost zero because currently conservation agriculture is most widely adopted in North and South America and Australia (Kassam et al., 2019) where agriculture tends to be mostly mechanized.

2.3 Preprocessing and statistical yield modeling

Before fitting the model, we pre-processed the data to allow for a robust statistical analysis. The following operations were carried out for each crop individually:

- The values for crop yield in kg per hectare in each cell represent a varying portion of the specific crop's harvested area ranging from 0.1 to 19,344.3 ha. This large range in crop area per cell size can influence the results of the analysis, as it gives each cell the same weight, independent of the actual agricultural area in the cell. Therefore, all rows containing values for harvested area below 100 ha were removed. This operation led to the deletion of 44-72% of all data points (depending on the crop, as do all following ranges shown). However, these cells contributed only between 1.6-3.2% of the total global crop production summed up over total crop specific harvested area and thus do not play an important part for global food security.
- Subsequently, missing values in the remaining datasets were addressed. Particularly the pesticides and mechanization data contained missing values. Gap filling of missing data, e.g. through interpolation, was not possible, as there is no established dependence of pesticides and mechanization on the other variables, so these data points were removed. In the N fertilizer column, missing values amounted to 1-2.3% of total data points. The temperature, the moisture regime and the soil/terrain related columns also had missing data points in the range of 1.6-2.2%. Cells with missing data for both data sets were treated with the forward filling method (carrying forward the last observed value).

N fertilizer, the manure, the pesticides and the yield contained implausible values. To prevent extreme outliers from skewing the relationship, all data with values above the 99.9th percentile for N fertilizer, manure (99th percentile), N total, pesticides and yield were removed. Given the distribution of the remaining values and the values commonly reported in the literature, these data points are more likely to be errors in the input datasets than real information characterizing the relationship between yield and input factors. Even though there is reason to assume that more values on both ends of the scale, albeit feasible, can be attributed to calculation errors or relics of the downsampling approach, this could not be validated and therefore, it was refrained from excluding more values. Additional information on the data cleaning process and

the effect of each operation on the metrics of the datasets can be found in reports/Report_descriptions.pdf and reports/Descriptive_statistics.xlsx in the repository of this paper (Moersdorf et al., 2023)).

In the next step, we check for any multicollinearity present in the data. It can be detected by calculating the variance inflation factor (Rawlings et al., 1998) for each predictor. The literature contains different threshold values for when the VIF indicates serious multicollinearity. The most prominent thresholds are specified as everything above 5 (Huang et al., 2010) or as values above 10 (Fox & Weisberg, 2011) constitute the need for action. However, the VIF does not work well for categorical variables if they have multiple levels. So instead, we compute the generalized variance inflation factor (GVIF) (Fox & Monette, 1992). To make it comparable across predictors with a differing number of levels, Fox and Monette (1992) suggest using $GVIF^{\frac{1}{2 \times Df}}$ with Df being equal to the number of levels in each variable. Squaring this value yields the regular variance inflation factor for predictors with one level, so that the variance inflation factor thresholds can be applied. The squared $GVIF^{\frac{1}{2 \times Df}}$ does not indicate any multicollinearity among the variables for any crop (see the Model_VIF sheet in reports/Model_results.xlsx in the repository of this paper (Moersdorf et al., 2023)).

As it is harder to maintain agricultural production in very cold, hot, dry or wet climates, an uneven distribution of observations among the levels in the thermal and moisture regime classes was detected. For the thermal regime the differences were particularly stark as the coldest three climate classes count with a very low number of observations. A highly uneven distribution of observations can lead the model to misjudge the significance of a predictor. To resolve the issue, the Temperate cool, Boreal and Arctic regimes were aggregated. The uneven distribution of observations in the moisture regime was addressed by fusing the two lowest (M1 and M2) and the two highest levels (M6 and M7) into one new level each: M2 = Length of Growing Period < 120 days and M6 = Length of Growing Period 270+ days. These merges do not reflect the best combinations for each crop. The wheat model, for example, could have benefitted from combining levels T1 and T2. However, we refrained from performing different merges for each crop to ensure comparability between the crops.

Adding the variables to the model consecutively does not show any abnormalities in the standard errors or the p values. Therefore, we estimated sufficient data quality for the following analysis.

A split-sample approach was applied to calibrate and validate the model. Prior to fitting the model, 20% of the pre-processed data were randomly selected. This sample was used for validation while the model was calibrated on the remaining 80% of the data points.

As the dependent variable cannot assume negative values, the distribution of the data points was strongly right skewed for all crops and the residuals were non-normally distributed, so the assumptions for a classic multiple regression on a normal distribution were violated. Therefore, a generalized linear model based on a gamma distribution was fitted to the data. The link function was assumed to be the natural logarithm, as the data showed a normal distribution at logarithmic scale. The model is specified as followed

$$Y \sim \text{Gamma}(\text{shape}, \text{scale})$$

where Y is the response variable that follows a gamma distribution, α is the shape parameter of the gamma distribution ($\alpha > 0$) and β is the scale parameter of the gamma distribution ($\beta > 0$). The expected value (mean) of the response variable (Y) μ can be written as an expression of shape and scale

$$\mu = \text{shape} * \text{scale}$$

The log link connects μ to the linear predictor η

$$g(\mu) = \ln(\mu) = \eta = \beta_0 + \beta_1 * x_1 + \beta_2 * x_2 + \dots + \beta_p * x_p \quad (\text{Eq1})$$

where $\beta_0, \beta_1, \beta_2, \dots, \beta_p$ are the model coefficients (parameters to be estimated), x_1, x_2, \dots, x_p are the predictor variables and p is the number of predictor variables.

The model was fitted with a simple linear relationship and no interactions. The categorical variables were coded as dummies. To assess model fit, we used McFadden's ρ^2 , which is an alternative for R^2 for non-normally distributed data. The significance level was set at $\alpha = 5\%$.

2.4 Yield prediction scenarios

Crop yields are projected under a worst-case scenario where the industry suffers significant losses, employing a generalized linear model. This assumes a global catastrophe that disrupts power supply, leading to the inhibition of industrial activities, communication, transportation, and other electricity-dependent services. However, it is presumed that transportation remains feasible to a certain extent, allowing farmers to receive necessary inputs and food distribution to continue (Abdelkhalik et al., 2016; D. C. Denkenberger et al., 2017). While the triggering event is expected to occur suddenly, the impact on agricultural production is likely mitigated by existing stocks of inputs in storage. Consequently, the aftermath of the catastrophe is divided into two phases: phase 1 encompasses the initial year, during which stocks are still available, while phase 2 commences in the second year when stocks are depleted, and the consequences of losing electrical infrastructure manifest in their entirety. The datasets used to calibrate the model's independent variables are adjusted for predictions based on the assumptions of either phase 1 or phase 2.

Phase 1

Phase 1 is meant to simulate the immediate stage after the catastrophe that caused the global catastrophic infrastructure loss. Phase 1 assumes the following:

- No irrigation reliant on electrical pumps.
- Full mechanization persists due to the availability of fuel.
- Reduced input of fertilizers and pesticides due to the cessation of production, although remaining stocks are utilized.
- Diminished availability of manure as animals are primarily slaughtered to prioritize food resources, retaining only those suitable for agricultural labor.

There should be enough fuel available to power agricultural machines for another year. The International Energy Agency (IEA, 2018) set the annual demand of the agricultural industry in oil products at 111,062 kt of oil equivalent (ktoe) in 2018. Available above-ground fuel after a

global catastrophic infrastructure loss was estimated at 319,000 ktoe, encompassing 172,000 ktoe of gasoline and 147,000 ktoe of diesel (Cole et al., 2016). Considering that most agricultural machinery runs on diesel, the estimated stocks last for about a year while leaving the gasoline for critical transportation. Thus, the mechanization input dataset remains unchanged for phase 1.

Nitrogen (N) fertilizer application rates for phase 1 are calculated based on the annual global nitrogen surplus (FAO, 2017). This is done under the assumption that not all fertilizer that is produced is used in the same year. They project a surplus of 14,477 kt N in 2020. In a first step we calculate the amount of the nutrient applied in each cell as a fraction of the total amount of the nutrient summed over the crop-specific harvested area with:

$$N_{frac} = \frac{N_{fert} \times A_{crop}}{\sum N_{fert} \times A_{crop}} \quad (\text{Eq2})$$

where N_{fert} is the application rate of the nutrient in $\text{kg ha}^{-1} \text{ cell}^{-1}$ and A_{crop} is the crop-specific harvested area in ha cell^{-1} . Each 5 arcminute cell has a specific application rate for N and a specific harvested area for each crop. The application rate is multiplied by the amount of crop area in each cell to determine the total amount of N applied to that cell. Then, this total is divided by the overall amount of N applied worldwide (the sum of N applied in all cells).

This division gives us a fraction, which represents the proportion of N applied to the entire world that each cell receives. In the first phase, when only a reduced amount of N is available, this reduction applies equally to each cell. So, if each cell used to apply 100 units of N under normal conditions, during Phase 1, they would only be able to apply 10 units of N because of the 90% reduction.

Then, we calculate the new total amount of the nutrient available for the specific crop $N_{total, crop}$ in phase 1 based on the surplus reported by the FAO (2017).

$$N_{total, crop} = \frac{\sum N_{fert} \times A_{crop}}{T_{NG}} \times T_{NG1} \quad (\text{Eq3})$$

where T_{NG} is the total amount of the nutrient (NG = nutrient global) projected to be used for crop fertilization in 2020 and T_{NG1} is the projected nutrient surplus in 2020. The total amount of N used for crop fertilization is projected to be 118,763 kt (FAO, 2017). Lastly the new total is allocated back to the cells based on N_{frac} :

$$N_{fert1} = \frac{N_{total, crop} \times N_{frac}}{A_{crop}} \quad (\text{Eq4})$$

The pesticide application rates for phase 1 are calculated with the same approach as the fertilizer application rates. However, no data were available on the production surplus of pesticides generated in one year. Therefore, it was assumed that the surplus' share of global pesticide production was in the same range as the share of the nutrients' surplus in the global nutrient production (around 10 %). Equations Eq2 and Eq4 were formulated accordingly for pesticides but remained structurally the same. The new total of pesticides $PE_{total, crop}$ available for a specific crop in phase 1 is calculated as follows:

$$PE_{total, crop} = \frac{\sum PE \times A_{crop}}{T_{PEG}} \times T_{PEG} \times \frac{\frac{T_{nG1}}{T_{nG}}}{2} \quad (\text{Eq5})$$

where PE is the pesticide application rate in $\text{kg ha}^{-1} \text{ cell}^{-1}$, T_{PEG} is the total amount of pesticides used (PEG = pesticides global) for agricultural purposes in 2019 (FAOSTAT, 2023b) and T_{nG1} and T_{nG} referring to the totals defined above for nitrogen.

Phase 2

In phase 2 all stocks are assumed to be depleted, hence, mechanisation_2 , n_{fert2} and PE_2 are set to zero.

Manure application rates are expected to be the same for phase 1 and 2 as they are dependent on the available livestock. It is assumed that the human population would switch to a mostly vegan diet to use the calories which can be produced in the most efficient way possible. Therefore, only draft animals like horses, buffaloes and cattle will be kept and fed on agricultural residues and roughage. For this analysis only cattle will be considered (Zhang et al., 2017). Zhang et al. (2017) did not include horses and buffaloes as they currently only constitute a very small percentage of the global livestock population and are even less important for manure production and application in modern agricultural systems. To calculate new manure application rates, the labor demand in each grid cell is assessed in terms of needed cattle per grid cell by dividing the harvested area in each cell by the area which can be worked by one head of cattle (ha per head of cattle), which is assumed to be 7.4 ha per draft animal as a typical working capacity (Prak, 2014). Considering that modern cattle are not bred to work, this value can be expected to be considerably lower. To be conservative in terms of manure availability, we used 5 hectares per head of cattle. Next, we calculated the excretion rate of one head of cattle. Zhang et al. (2017) provided the total amount of manure produced in 2014 which amounts to 131,000 kt N and the share of the manure produced by cattle, namely 43.7%. There were 1.44 billion head of cattle in 2014 (FAOSTAT, 2023a). Multiplying the total amount of manure with the fraction attributed to cattle and dividing the result by the heads of cattle in that year rendered an excretion rate of $\sim 40 \text{ kg N head}^{-1} \text{ yr}^{-1}$. In the last step the new crop specific N manure application rate M_{nC} was computed by

$$M_{n, crop} = \frac{39.77 \times C_{crop}}{A_{crop}} \quad (\text{Eq6})$$

where C_{crop} is the crop specific number of cattle in each grid cell. This means that the available manure comes from the draft cattle needed to labor the area in that cell.

For phase 1 $M_{n,crop}$ was combined with n_{fert1} into n_{tot1} . In phase 2 the N from manure is the only source of N left, so it is taken as the sole input.

As with manure, irrigation as a fraction of the cropland in a cell which is actually irrigated cannot profit from first year stocks and therefore the same values are used for phase 1 and phase 2. A sharp reduction in actually irrigated area is expected as large parts of the irrigation infrastructure are dependent on electricity and fossil fuels. Today, around 20 % of cultivated land is irrigated and it contributes 40 % of global food production. To obtain the fraction of irrigated area which is reliant on electricity, we combined the information on the source of the irrigation water (surface or groundwater or other) with country-level statistics. The fraction of actually irrigated cropland in a global catastrophic infrastructure loss (GCIL) scenario I_{gcil} was calculated as follows:

$$I_{gcil} = I_{AC} \times (1 - I_{RC}) \quad (\text{Eq7})$$

where I_{AC} is the total currently (AC = all currently) irrigated fraction of cropland in each cell and I_{RC} is the fraction of currently irrigated area which is reliant (RC = reliant currently) on electricity or diesel in each cell.

The datasets comprising the input variables for phases 1 and 2 are fed into the model specified above to predict the crop-specific yields under global catastrophic infrastructure loss conditions. The predicted values are used to calculate the crop-specific relative change in yield RC_C for each cell:

$$RC_{crop} = \frac{(Y_{PC} - Y_{crop})}{Y_{crop}} \quad (\text{Eq8})$$

where Y_{PC} is the predicted crop-specific (PC) yield in the respective phase 1 or 2 and Y_{crop} is the crop-specific yield around 2010 taken from the SPAM2010 dataset. Values above zero, resulting from the generalized linear model, were set to zero as yield increase in a global catastrophic infrastructure loss scenario is not realistic. Rather, the positive values are taken as an indication for stable yields unaffected by catastrophic circumstances. For the predicted yield and relative change, descriptive statistics measures were computed for each phase and crop, namely the range of values, the total crop production, the weighted mean and the corresponding confidence interval. The weighted mean was also calculated for each continent. The yield was weighted according to the corresponding harvested area while the relative change was weighted according to the crop production in 2010. The results of and additional information on these calculations can be found in reports/Report_descriptions.pdf and reports/Prediction_statistics.xlsx in the repository of this paper (Moersdorf et al., 2023)).

3 Results

3.1 Model calibration and validation

A generalized linear model based on a gamma distribution with a log link was fitted for all crops using the same set of variables. The final model for each crop incorporated the explanatory variables listed in Table 2. Most coefficients had, as anticipated, a positive impact on the expected yield, but the model struggled to accurately capture low yield values. Nearly all coefficients were statistically significant at a 5% significance level, except for three instances: In the wheat model, the thermal regime level 2 was not significantly different from level 1 and the moisture regime level 3 was not significantly different from level 2; in the soybean model the nitrogen input did not have a significant impact. For soybean, nitrogen application was not a significant yield influencing factor as it is a leguminous plant which is able to fix nitrogen. Wheat is not a crop that is routinely grown under tropical conditions. Therefore, it is reasonable that the different tropical climates (T1 + T2, M2 + M3) result in similar yields and do not show significant differences from each other. Further, the thermal and the moisture regime levels were combined due to low numbers of data points in extreme climates. However, the same number of levels was used for all crops to ensure model comparability between crops. Consequently, it does not reflect the ideal number of levels for each individual crop: for wheat, for example, the number of observations in T1 and T2 was very low, so they could have been combined into one class. Nonetheless, the separation was maintained to ensure consistency with the models for corn, rice, and soybean.

Table 2: List of independent variables used in the generalized linear model.

Variable	Description	Categorical/ Continuous	Unit/Categories
n_total	Total nitrogen input (includes fertilizer and manure input)	Continuous	kg/ha
pesticides	Cumulated pesticide input (contains 20 different substances, see Table 1)	Continuous	kg/ha
irrigation_tot	Fraction of irrigated cropland per cell	Continuous	Unitless, values between 0 and 1
mechanized	Use of agricultural machinery for farming activities	Categorical	0=not mechanized; 1=mechanized
thz_class	Thermal regime class	Categorical, dummy-coded	T1=Tropics, lowland; T2=Tropics, highland; T3=Subtropics, warm; T4=Subtropics, moderately cool; T5=Subtropics, cool; T6=Temperate, moderate; T7=Temperate, cool, Boreal + Arctic
mst_class	Moisture regime class	Categorical, dummy-coded	M2=Length of Growing Period(LGP) < 120 days; M3=LGP 120-180 days, M4=LGP 180-225 days; M5=LGP 225-270 days; M6=LGP > 270 days
soil_class	Soil/terrain-related class	Categorical, dummy-coded	S1=Dominantly very steep terrain; S2=Dominantly hydromorphic soils; S3=No or few soil/terrain limitations; S4= Moderate soil/terrain limitations; S5=Severe soil/terrain limitations; L3=Irrigated soils

We measured the total yield change per factor by comparing the minimum and maximum input values while keeping other factors constant (see sheet YieldReductionPerFactor in reports/Model_results.xlsx) (Figure 1). This difference was expressed as a percentage of the maximum input's yield, indicating the extent of yield change when the respective factor was absent. The most influential factor varied with the crop type. For corn, irrigation caused a significant 40% yield decrease. Total nitrogen application rate had the largest impact on rice and wheat yields, resulting in a 45% reduction. In contrast, soybean yield was most affected by the use of machinery, with a 36% decrease. Pesticide application had the lowest effect, notably impacting only wheat yields with a 39% reduction. Interestingly, rice yields showed an unexpected relationship with pesticide application. The model estimated a yield increase of over 10% when no pesticides were used (this is discussed in chapter 4.2). Overall, irrigation had the most substantial negative impact on yields for three crops, followed closely by the use of agricultural machinery. Nitrogen application had a varying impact, causing the highest reduction for wheat and rice, while its effect on rice was relatively low (18% decrease) and negligible for soybean.

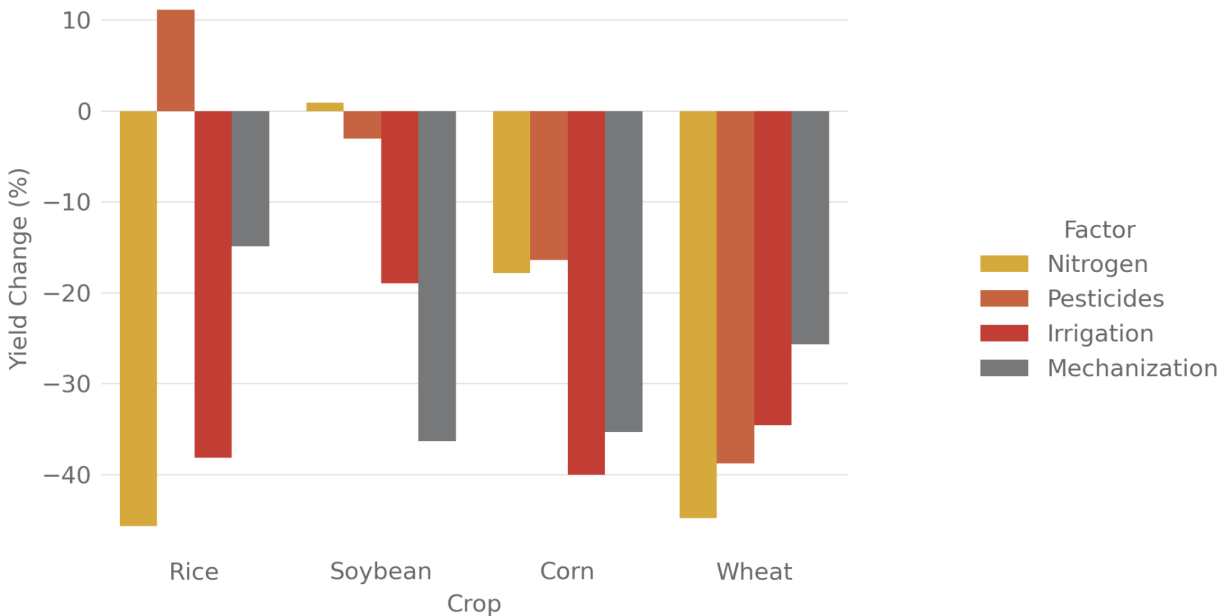


Figure 1: Projected yield change based on the difference between the maximal and minimal value for all factors by crop.

To calibrate the models, 80% of the data points were used, while the remaining 20% were reserved for validating the model fit using McFadden's ρ^2 . The validated ρ^2 -values exhibited strong variation across different crops, with the highest agreement between data and model found for corn, yielding a ρ^2 of 0.47. The generalized linear model for rice achieved a ρ^2 of 0.40, while the wheat model obtained 0.36, and the lowest value was observed for soybean at 0.32.

Nonetheless, all validation values indicated a good fit of the models to the data, as ρ^2 values ranging from 0.2 to 0.4 represent an excellent fit according to McFadden (1977).

The detailed model results for each crop including a 95% confidence interval for the coefficients and the corresponding goodness of fit metrics can be accessed in reports/Model_results.xlsx in the repository of this paper (Moersdorf et al., 2023)).

3.2 Mean predicted yield and average yield reduction in a global catastrophic infrastructure loss scenario

The predicted yields show significant variation between phase 1 and 2, as well as across different crops and continents (Figure 2, 3). In phase 1, the average reduction by crop is between 15 and 37%, while in phase 2, it increases to values between 35 to 48% (Figure 2). Among all the crops, soybeans experience the smallest reduction overall, especially in phase 1. The reductions differ greatly between phase 1 and 2 for all crops except rice. Rice yield reduction increases from 32% in phase 1 to 35% in phase 2. In contrast, soybeans perform relatively well in phase 1 but experience a large decrease in phase 2 (from 15% to 42% yield reduction). Both wheat and corn already exhibit substantial yield reductions in phase 1 (37% and 30% respectively), which further worsen in phase 2 (48% for both).

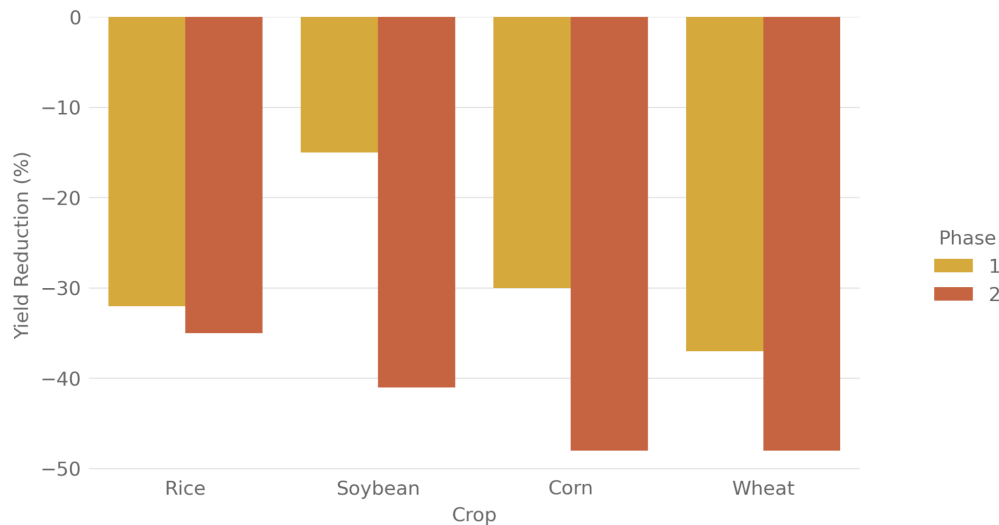


Figure 2: Projected yield reduction for phase 1 and 2 by crop. Values are weighted by the production of the cells (area times yield), as those areas are more important for food security.

The magnitude of yield decrease also varies significantly by continent (Figure 3). Africa has the lowest average yield reduction, around 26% over both phases, with little difference between the phases. Asia also shows a small disparity between phase 1 and 2, but the average yield reduction over both phases is at 32% notably higher compared to Africa. The difference between phase 1 and 2 is more pronounced in the remaining continents where yield decreases by at least two thirds from phase 1 to phase 2. Europe and South America face a similar reduction of approximately 25% in phase 1 and 44% in phase 2. With a projected decrease in yield of around 30% in phase 1 and almost 48% in phase 2, North America and Oceania are most severely affected.

The detailed prediction results for each crop, phase and continent and, for comparison, also the metrics for the yield under current conditions are provided in reports/Prediction_statistics.xlsx in the repository of this paper (Moersdorf et al., 2023). For further information on all plots presented in this work and their accompanying metrics, reports/Reports_descriptions can be consulted.

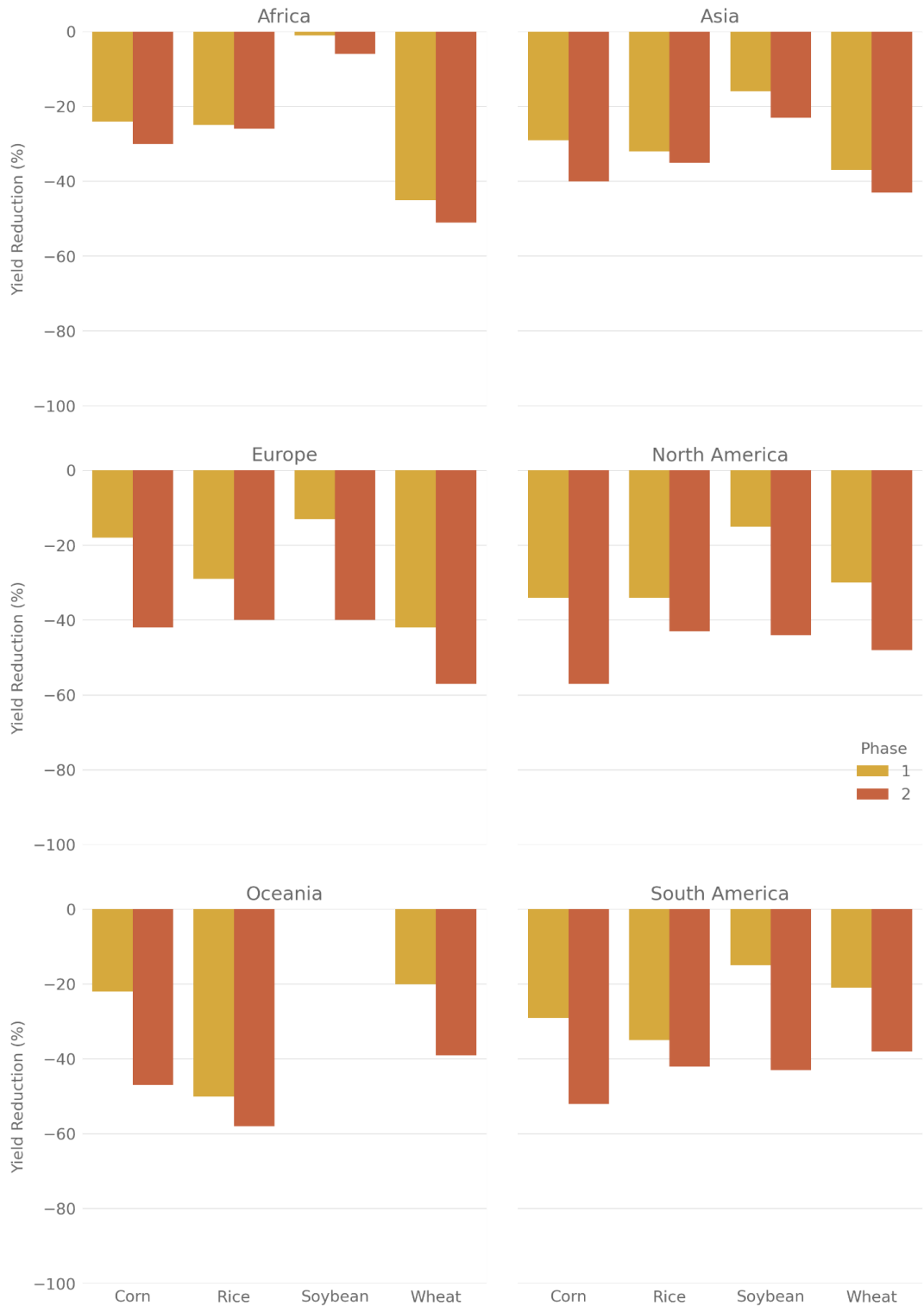


Figure 3: Projected yield reduction for phase 1 and 2 and all crops by continent. Values are weighted by the production of the cells (area times yield), as those areas are more important for food security.

3.3 Spatial patterns of yield loss

The predicted yield loss reveals distinct hotspots in corn (Figure 4), rice (Figure 5), soybean (Figure 6) and wheat (Figure 7). The impact is more severe in Phase 2, as it represents the full consequences of losing industrial inputs. Based on the generalized linear model, corn yields are projected to suffer significant reductions in North and South America, Europe, South Africa, Zambia, the Nile region, and Southern India. In China, Indonesia, and other parts of India, the reaction to the impact is highly heterogeneous, with regions alternating between strong and minimal effects, which reflects the heterogeneous distribution of small holder and large scale agriculture there today. Similar heterogeneity is observed in India and China for soybean yields, in Indonesia for rice yields, and in Central China, the Southwestern Caspian region, and Ethiopia for wheat yields.

Rice yield loss hotspots are projected to be in China, India, Southern Brazil, the Mississippi region, and European rice-growing regions. Soybean yields are expected to be most diminished in North and South America and Central Europe. For wheat, the largest decrease in yield is predicted in Europe, North America, South Africa, Argentina, Northern India, Northeastern China, Southern Australia, and the Nile region. Globally, the areas with the most significant negative impacts on yields are anticipated to be North and South America, Europe, China, India, and Indonesia. These reductions directly align with the level of industrialization in agriculture today.

When considering the combined implications of these maps, it becomes apparent that significant agricultural regions, such as Central Europe, are projected to endure a substantial decline of up to 75% in their production potential for rice, wheat, soybean, and corn. Less intensely farmed areas exhibit lesser impact, but are also usually less productive under current conditions.

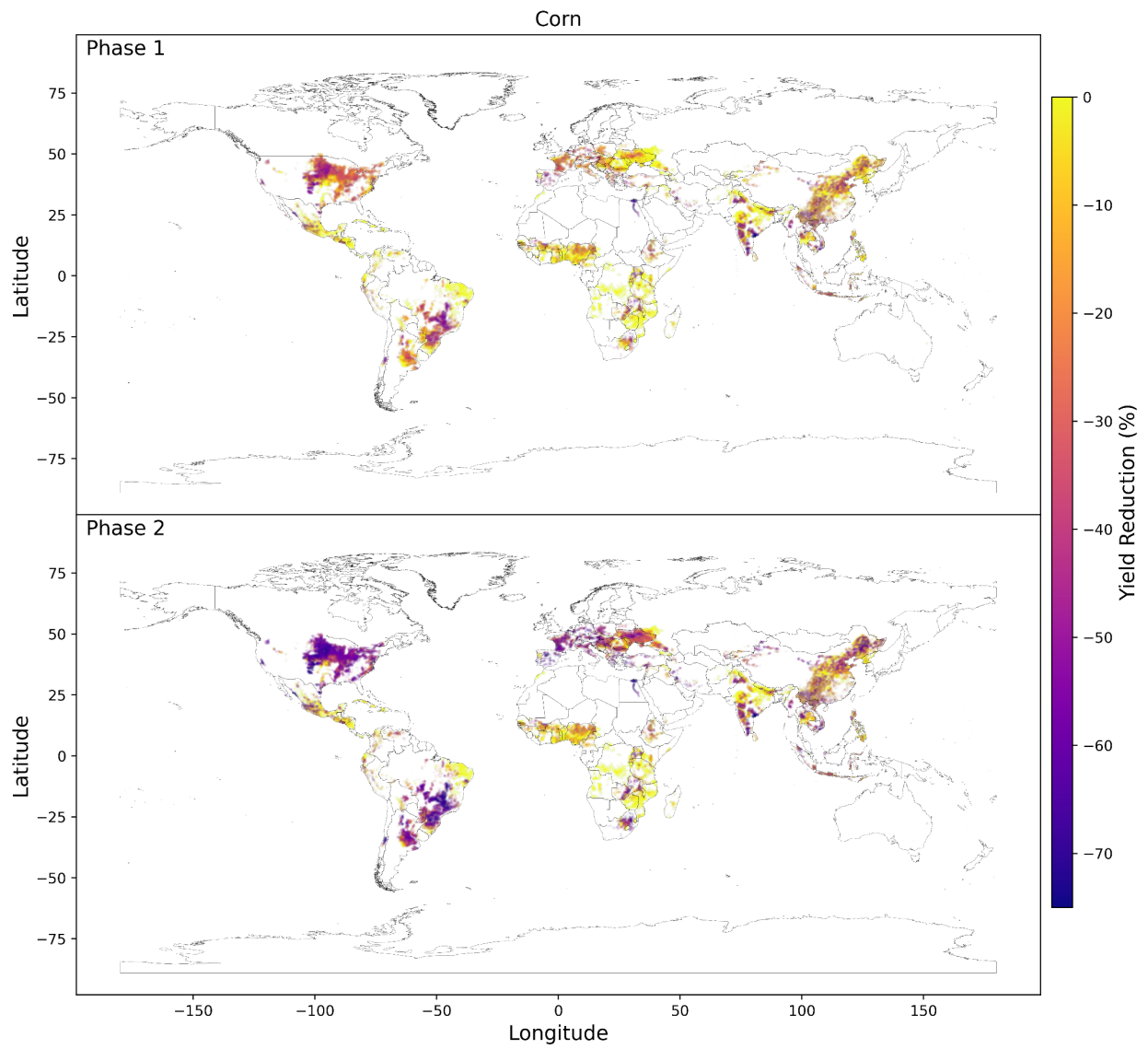


Figure 4: Spatial distribution of yield loss for corn in phase 1 and 2 at a resolution of 5 arcmin.

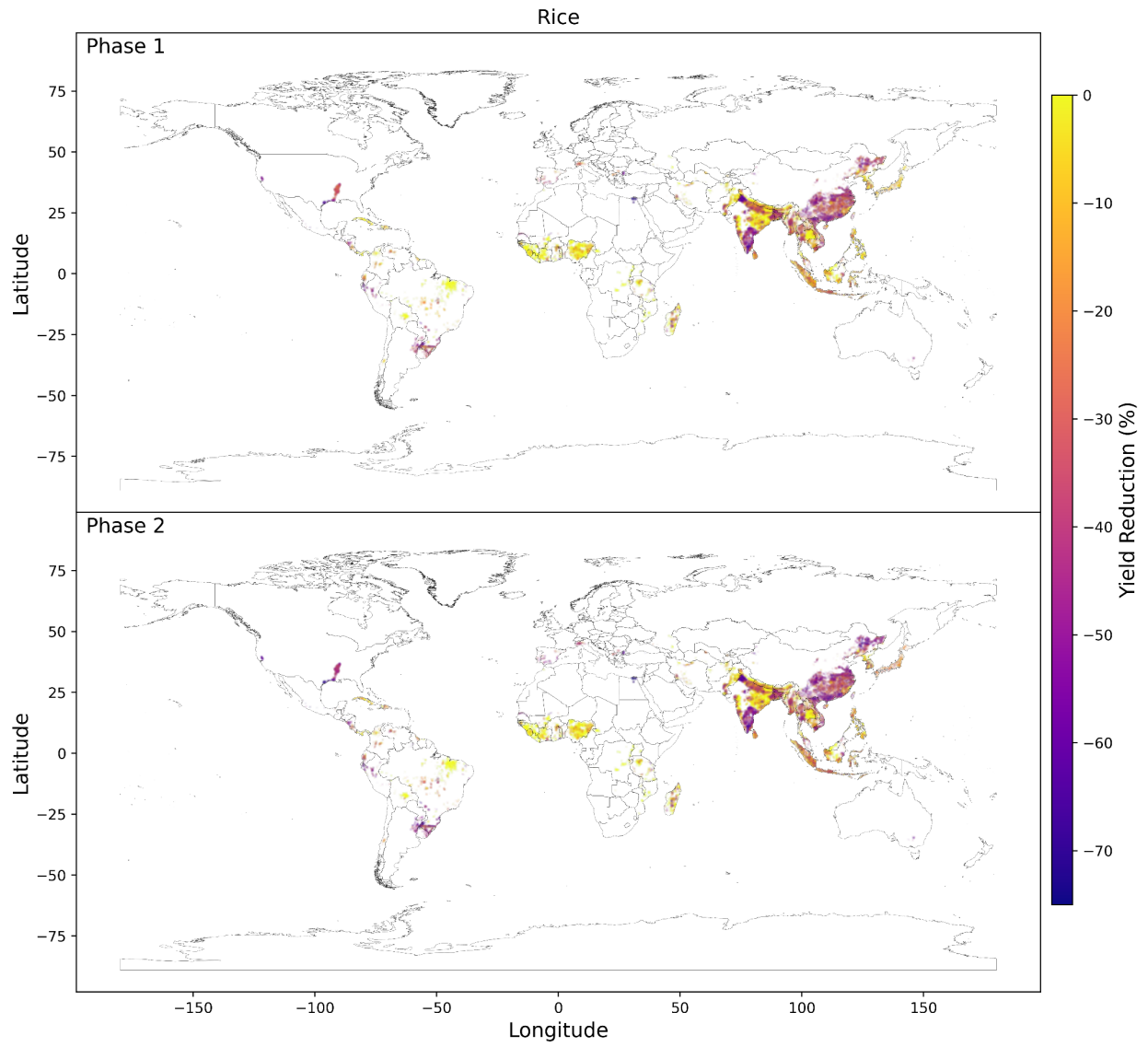


Figure 5: Spatial distribution of yield loss for rice in phase 1 and 2 at a resolution of 5 arcmin.

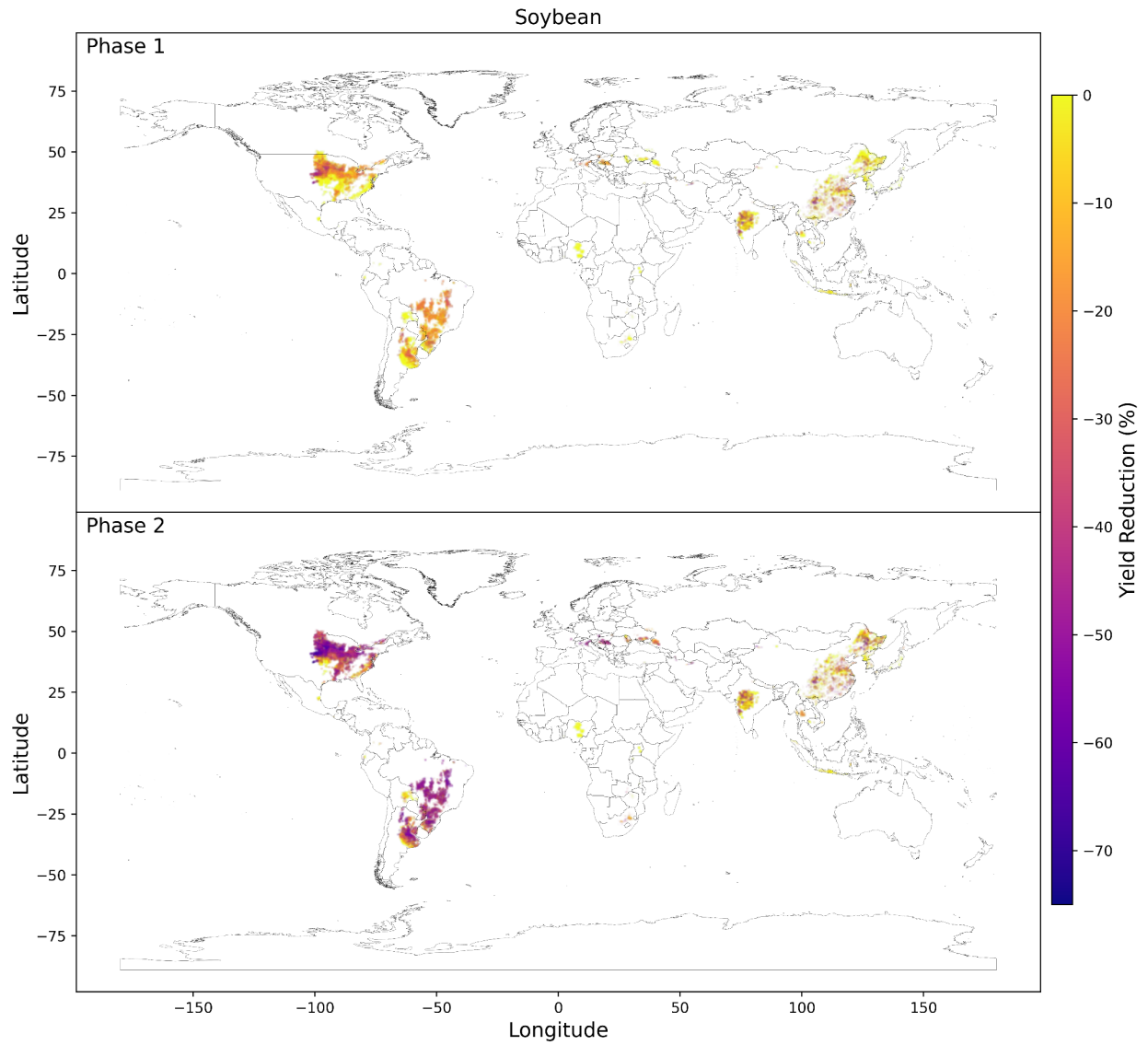


Figure 6: Spatial distribution of yield loss for soybean in phase 1 and 2 at a resolution of 5 arcmin.

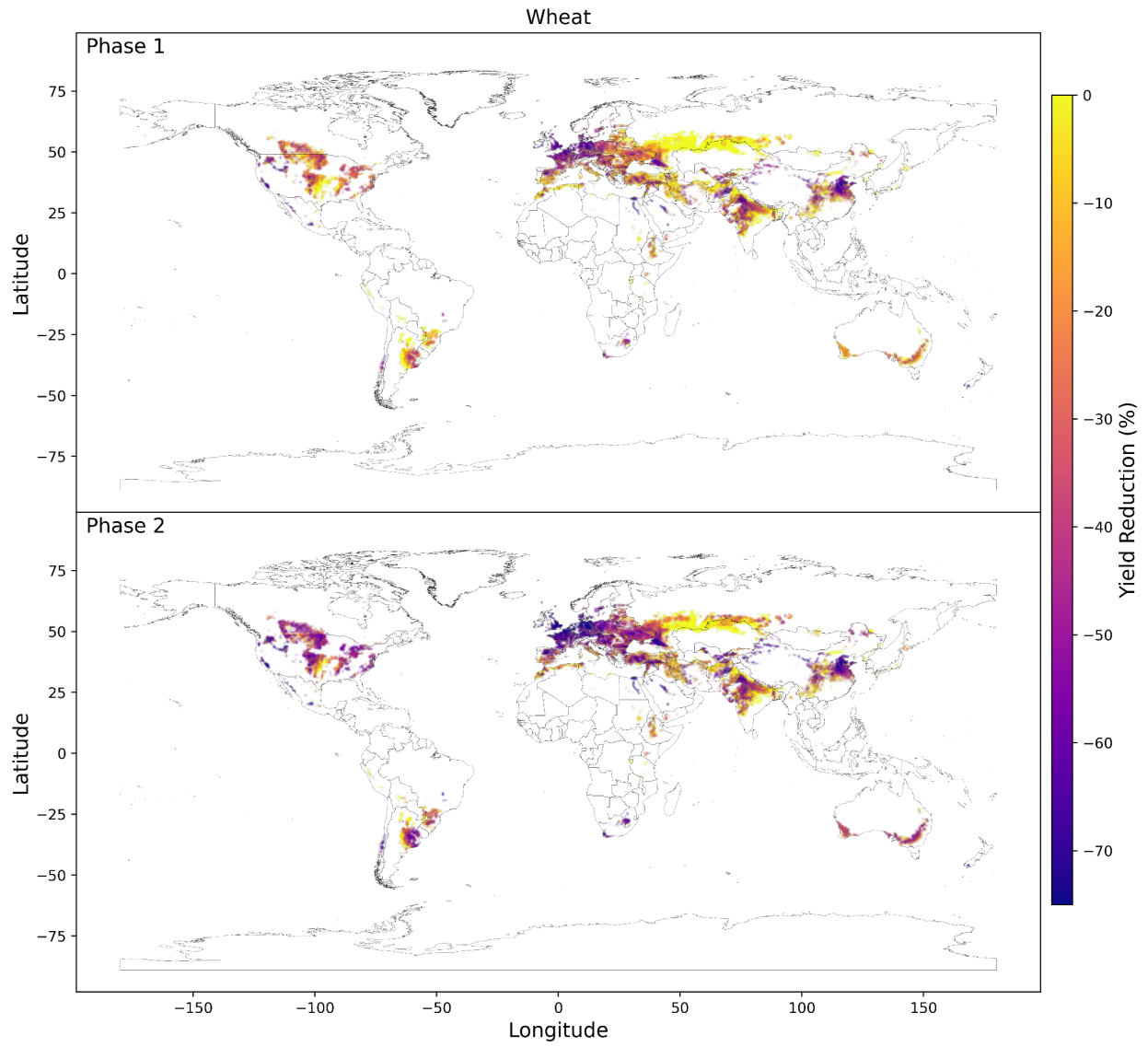


Figure 7: Spatial distribution of yield loss for wheat in phase 1 and 2 at a resolution of 5 arcmin.

4 Discussion

Following the first evaluations of the possible effects of a global catastrophic infrastructure loss scenario on agriculture by Cole et al. (2016) this work proposes a formal modeling approach to investigate the issue, adds a spatial component to the analysis and examines global catastrophic infrastructure loss consequences on agriculture in two different phases. Cole et al. (2016) assume pre industrial agricultural yield in a global catastrophic infrastructure loss scenario which corresponds to a 60% drop from current yield levels. The results at hand suggest that overall yields would only drop by around 35 to 48 % depending on the crop in phase 2, with corn and wheat (-48 % in phase 2) experiencing the largest reduction. However, areas with highly industrialized agriculture are affected much more severely and local yield reductions can reach 75% and more. Still, while Cole et al. (2016) describe their yield estimate as conservative, the results presented above can be considered optimistic. Due to data availability we were not able to include all relevant factors and most of the omitted factors would likely decrease yield even more. Therefore, the predictions should be understood as a first crop-specific and spatially explicit estimate on how strongly yields could be affected by a catastrophic scenario which inhibits global industry. The general trends visible in the prediction results are reliable and can be used as a guideline going forward.

4.1 Limitations

The Input datasets for fitting the generalized linear model were carefully selected, and each represent a highly significant influence factor as was confirmed by the model results. The high resolution of five arcminutes was chosen to sufficiently capture the heterogeneity of agricultural production. However, there are several shortcomings in the available data. First and foremost, the datasets do not actually showcase the real distribution of the specific variables but rather a statistical approximation of the real distribution by downsampling. This introduces uncertainties, which are consequently replicated in our model. The datasets used in this analysis were not harmonized against each other and standardization was only exercised by some on the country level against FAOSTAT data. In consequence, the layers do not necessarily fully align: they differ in the extent covered and in the spatial distribution.

Discrepancies in the extent result in missing data points in the combined dataset used in the analysis. The mechanized and pesticides datasets covered substantially fewer cells than the remaining ones. This resulted in many cells having to be dropped before calibrating the model (Additional information on the data cleaning process and the effect of each operation on the metrics of the datasets can be found in reports/Report_descriptions.pdf and reports/Descriptive_statistics.xlsx in the repository of this paper (Moersdorf et al., 2023)). This was especially a problem in Africa. Solely the corn generalized linear model was calibrated on sufficient points for that region to yield viable results for most of the African continent. This coincides with the uncertainty reported by Yu et al. (2020) as they estimate that the uncertainty of the SPAM2010 dataset is highest in Africa. Apart from the cumulation in African countries, the dropped cells concentrate outside of the main growing regions and therefore also count with small harvested areas for the respective crop. Hence, even though many cells were dropped before calibrating the model, the remaining data still represent the main growing regions and the majority of yearly crop production for each crop. For rice and soybean the excluded cells concentrate in Europe and Central America and for rice also in South America. Corn and wheat

overall count with less and smaller clusters of excluded cells as both have major growing zones in most regions of the world.

Another consequence of misalignment between input datasets has more severe effects on the model accuracy: If the spatial distribution of values does not match across datasets, the relationship between the variables we are trying to study (dependent and independent) may be misrepresented. Consequently, the fundamental subject of our analysis could be distorted. However, we mitigated this issue by working with large datasets to ensure a sufficient overlap to properly map the relationship.

Due to the spatial nature of the analyzed data the yield value in each cell does not simply represent one unit but is rather tied to the area in each cell where the crop is harvested. As a result, yield values in cells with large harvested areas have a higher importance for the overall crop yield production than values with smaller harvested areas. A standard generalized linear model, however, attributes the same weight to each data point, assuming that each data point stands for one observation. This leads to yields in small areas having a disproportionately large influence on the model relative to the area they cover while yields on large areas carry proportionately less weight. To address this imbalance by narrowing the range of the harvested area values, cells containing less than 100 ha of harvested area were excluded from the modeling dataset.

Working with spatial data can also lead to effects of autocorrelation among data points. In high resolution datasets which are derived from statistical interpolation, the effect is enhanced as more cells in close vicinity to each other tend to contain the same value. Considering that classical generalized linear models are not equipped to handle this relationship, autocorrelation can skew model results, especially in combination with misaligned data sets.

While autocorrelation is a phenomenon within one factor, multicollinearity occurs between two or more independent variables. Initially, we intended to include the phosphorus fertilizer application rate as a model factor. High quality data were available from the same source as the nitrogen fertilizer application rate. This, however, led to multicollinearity between the datasets which had a noticeable impact on the model results. Oftentimes, nitrogen and phosphorus (and potassium) are applied as compound fertilizer. Therefore, we decided to consider the nitrogen application rate as a proxy for nutrient input in general and to move forward without the phosphorus application rate.

As pointed out in 3.1, the fitted models struggle with accurately capturing low yields and overall estimate a more moderate range of values than the training data (see reports/Prediction_statistics.xlsx). Especially for low yields this leads to interpretation problems for the yield reduction: The predicted minimum value is at least eight times higher than in the SPAM2010 dataset, so all data points with lower values in the original dataset are projected to experience a yield increase in a global catastrophic infrastructure loss scenario. That is highly unrealistic as the catastrophe will have lasting effects on society as whole, creating conditions which render the improvement of marginal yields very unlikely. Among the model estimates for different conditions, we also observe that unlike the maximum values, the minimum values barely differ within one crop. This suggests that lower yields are only marginally if at all negatively affected by global catastrophic infrastructure loss. We take this as an indication for stable yields under catastrophic conditions and therefore, interpret yield increases as yield retention, i.e. no change in yield. There are multiple possible reasons for the smaller value range

in model estimates. Generally, a log link tends to smooth out extremes to be able to generate better estimates for new data, especially if the training data feature a lot of noise from outliers. It is likely that the SPAM2010 data contain more outliers on both ends of the spectrum than we have addressed during the data cleaning process. Additionally, the relationship between dependent and independent variables could be skewed due to data misalignment (see above). The effect is likely stronger in the extremes where less data points are available to map the relationship. Finally, as explained in 2.1 and discussed in 4.2, we had to leave out possibly highly relevant variables due to lack of data which can also lead to an inaccurate model fit.

The models for rice and soybean each estimated a negative relationship between one agricultural input and the crop yield. This is unexpected as substances are generally applied to benefit crop production. For soybean, nitrogen application had a slightly negative effect on crop yield. While not necessarily expected, this is no reason for concern as this factor is not statistically significant and soybean is able to fix nitrogen from the air. The notably stronger, statistically significant negative effect size of pesticide application for rice on the other hand is surprising. This coefficient does not accurately portray the relationship between pesticide application and rice yields and there are several possible reasons for the misrepresentation. First, it could also result from the misaligned data: The rice and soybean datasets have fewer data points than corn and wheat so it might not suffice to accurately map the relationship despite the misaligned values. Further, the data quality is typically better in Europe and North America and the rice and soybean datasets do not have major growing areas in those regions. Lastly, the relationship between pesticide and nitrogen application rates and yield were calibrated on smaller units than irrigation and mechanized. As a result, the relationship is less pronounced.

Still, the results here can be seen as a good first estimate of the effects of a global catastrophic infrastructure loss scenario and should be refined further in the future. The spatial distribution of yield loss maps very well with the expectation that highly industrialized agriculture would suffer the most.

4.2 Implications of a global catastrophic infrastructure loss scenario

The results demonstrate a substantial difference between phase 1 and phase 2 yield losses. It shows that phase 1 can be critical in the preparation for phase 2 because the yield losses are more manageable in the first phase. This can provide the time necessary to adapt to the new circumstances by building up non-electrical logistic infrastructure, building tools and wagons, establishing a communication system, implementing new farming techniques and crop rotations to manage pests and nutrients, and overall adjusting as a society. The crucial component is the continued use of the agricultural machinery as it ensures that tasks can be completed on large farms even as the preparations for the transition to a human and animal operated system are still underway.

Due to limited data availability some of the factors that were identified as important for estimating yields in a global catastrophic infrastructure loss scenario were not included in the generalized linear model: seed availability, (dominant) variety and knowledge of farmers. Beyond these potential model input factors, there are other characteristics of a global catastrophic infrastructure loss scenario which codetermine the availability of the input variables in case of a catastrophe: availability of feed for draft animals and tools and materials for draft work, draft animals' constitution, population relocation, climate change, alternative pest control methods, crop rotations, alternative nutrient sources, means to conserve food and the time it

takes to slaughter an animal. All listed factors and aspects have the potential to increase or decrease the crop yield in a global catastrophic infrastructure loss scenario. Nonetheless, most are likely to worsen the catastrophic impact.

Likely the three most important factors are: Seed availability, dominant variety and the ability of farmers to cope with such a massive shift in production techniques. Seed availability and the distribution of crop varieties are closely interlinked. A large share of farmers, especially in industrialized countries, purchase their seeds from large global companies and do not retain seeds from their own harvest for the next year. This could be changed if needed but still, these varieties are oftentimes specifically bred to grow well in high-input conditions and to be bought again. This does not mean that these seeds will not grow, nor will they necessarily grow badly under low input conditions, but they are certainly more prone to crop failure than local landraces (Mikkelsen & Bruulsema, 2005). In a global failure of electrical infrastructure, highly specialized and industrialized plant breeding and seed production will likely also be disrupted. Corn would be particularly strongly affected as almost all corn crops are grown from hybrid seeds which are bred varieties targeted specifically at a high one-year performance. If there are no seeds available from large seed companies and the seeds saved from the high-yielding varieties do not perform well in the global catastrophic infrastructure loss scenario, there will not be sufficient seed from landraces available to cultivate all of the current cropland area. Switching from highly mechanized agriculture to traditional farming techniques may present a challenge for many farmers. However, there are still some small farms that continue to employ traditional knowledge. These farms can serve as a valuable resource for teaching farmers the traditional techniques once again.

5 Conclusions

The goal of this study was to gain new insights into the impact of a large-scale industrial outage caused by a global catastrophe on the yields of corn, rice, soybean, and wheat. It presents the first crop-specific and spatially explicit estimation of the effect on crop yields for two different phases of the scenario, each varying in severity.

Based on the findings, we can conclude that the effects are not uniform across regions, with clear distinctions between strongly affected and minimally affected areas. The identified hotspots differ for each crop, aligning with the primary growing regions and the level of industrialization in agriculture.

Notable differences were also observed between phase 1 and phase 2. The presence of available stocks of agricultural inputs, although representing only a fraction of the current annual use, played a crucial role in mitigating yield losses. Phase 1 was identified as a critical step in allowing agriculture to adapt to the new conditions with changes like using more manure. Another critical adoption would be a change to a mostly vegan diet. This would free up enough calories to counteract a part of the experienced losses and enable a larger part of the population to rebuild infrastructure.

Moving forward, future research should focus on refining the estimates by either improving the statistical approach presented in this study or integrating a statistical framework with machine learning techniques or process-based crop models. The analysis could also be expanded to include a wider range of crops and other agricultural inputs. Additionally,

conducting region-specific analyses, particularly in the identified hotspots and in Africa, could provide valuable insights.

Acknowledgments

We would like to thank Dr. Christina Ramsenthaler and Dr. Ruslan Krenzler for helping us with statistical analysis. A special thank you goes to Hans Hartwig Lützow and the Untermühlbachhof, who kindly provided us with much hands-on information on how cattle can be trained as draft animals. Finally, we would like to thank Mariana Antonietta and Juan B. García Martínez for providing us with valuable feedback to this manuscript.

ALLFED acknowledges funding from the Survival and Flourishing Fund.

Author Contribution

- Conceptualization: JM, DD, FUJ
- Data curation: JM, MR
- Formal analysis: JM, MR, FUJ
- Investigation: JM, FUJ
- Methodology: JM, MR, FUJ
- Project administration: DD, FUJ
- Resources: DD, LB
- Software: JM, MR, FUJ
- Supervision: DD, FUJ
- Writing - original draft: JM, FUJ
- Writing - review and edit: JM, MR, DD, LB, FUJ

References

- Abdelkhalik, M., Denkenberger, D., Griswold, M., Cole, D. D., & Pearce, J. (2016, August 28). *Providing Non-food Needs if Industry is Disabled*. IDRC DAVOS 2016. Integrative Risk Management - Towards Resilient Cities. <https://hal.science/hal-02113489>
- Alston, J. M., & Pardey, P. G. (2014). Agriculture in the Global Economy. *Journal of Economic Perspectives*, 28(1), 121–146. <https://doi.org/10.1257/jep.28.1.121>
- Alvarado, K. A., Mill, A., Pearce, J. M., Vocaet, A., & Denkenberger, D. (2020). Scaling of greenhouse crop production in low sunlight scenarios. *Science of The Total Environment*, 707, 136012. <https://doi.org/10.1016/j.scitotenv.2019.136012>
- Avin, S., Wintle, B. C., Weitzdörfer, J., Ó hÉigeartaigh, S. S., Sutherland, W. J., & Rees, M. J.

- (2018). Classifying global catastrophic risks. *Futures*, *102*, 20–26.
<https://doi.org/10.1016/j.futures.2018.02.001>
- Baum, S. D. (2023). Assessing natural global catastrophic risks. *Natural Hazards*, *115*(3), 2699–2719. <https://doi.org/10.1007/s11069-022-05660-w>
- Baum, S. D., Denkenberger, D. C., Pearce, J. M., Robock, A., & Winkler, R. (2015). Resilience to global food supply catastrophes. *Environment Systems and Decisions*, *35*(2), 301–313.
<https://doi.org/10.1007/s10669-015-9549-2>
- Bostrom, N., & Cirkovic, M. M. (2008). *Global Catastrophic Risks*. Oxford University Press, Oxford.
- Cao, B., Yu, L., Li, X., Chen, M., Li, X., Hao, P., & Gong, P. (2021). *A 1 km global cropland dataset from 10000 BCE to 2100 CE (Version 1)* [dataset]. Zenodo.
<https://doi.org/10.5281/zenodo.5105689>
- Cliver, E. W., Schrijver, C. J., Shibata, K., & Usoskin, I. G. (2022). Extreme solar events. *Living Reviews in Solar Physics*, *19*(1), 2. <https://doi.org/10.1007/s41116-022-00033-8>
- Coates, J. F. (2009). Risks and threats to civilization, humankind, and the earth. *Futures*, *41*(10), 694–705. <https://doi.org/10.1016/j.futures.2009.07.010>
- Cole, D. D., Denkenberger, D., Griswold, M., Abdelkhalik, M., & Pearce, J. (2016, August). Feeding Everyone if Industry is Disabled. *IDRC DAVOS 2016 Integrative Risk Management - Towards Resilient Cities*. <https://hal.archives-ouvertes.fr/hal-02113486>
- Cooper, C., & Sovacool, B. K. (2011). Not Your Father's Y2K: Preparing the North American Power Grid for the Perfect Solar Storm. *The Electricity Journal*, *24*(4), 47–61.
<https://doi.org/10.1016/j.tej.2011.04.005>
- Denkenberger, D. C., Cole, D. D., Abdelkhalik, M., Griswold, M., Hundley, A. B., & Pearce, J.

- M. (2017). Feeding everyone if the sun is obscured and industry is disabled. *International Journal of Disaster Risk Reduction*, 21, 284–290.
<https://doi.org/10.1016/j.ijdr.2016.12.018>
- Denkenberger, D., Sandberg, A., Tieman, R. J., & Pearce, J. M. (2021). Long-term cost-effectiveness of interventions for loss of electricity/industry compared to artificial general intelligence safety. *European Journal of Futures Research*, 9(1), 11.
<https://doi.org/10.1186/s40309-021-00178-z>
- Diamond, J. M. (2011). *Collapse: How societies choose to fail or survive*. Penguin Books.
- Evenson, R. E., & Gollin, D. (2003). Assessing the Impact of the Green Revolution, 1960 to 2000. *Science*, 300(5620), 758–762. <https://doi.org/10.1126/science.1078710>
- FAO. (2017). *World fertilizer trends and outlook to 2020: Summary Report*. FAO.
<https://www.fao.org/documents/card/en?details=cfa19fbc-0008-466b-8cc6-0db6c6686f78>
/
- FAO. (2019). *AQUASTAT Core Database. Food and Agriculture Organization of the United Nations*. [dataset].
https://tableau.apps.fao.org/views/ReviewDashboard-v1/country_dashboard?%3Adisplay_count=n&%3Aembed=y&%3AisGuestRedirectFromVizportal=y&%3Aorigin=viz_share_link&%3AshowAppBanner=false&%3AshowVizHome=n#1
- FAOSTAT. (2023a). *Crops and livestock products* [dataset].
<https://www.fao.org/faostat/en/#data/QCL>
- FAOSTAT. (2023b). *Global Pesticide Use* [dataset]. <https://www.fao.org/faostat/en/#data/RP>
- Fischer, G. (2021). *Global Agro-Ecological Zones v4 – Model documentation*. FAO.
<https://doi.org/10.4060/cb4744en>

- Fox, J., & Monette, G. (1992). Generalized Collinearity Diagnostics. *Journal of the American Statistical Association*, 87(417), 178–183. <https://doi.org/10.2307/2290467>
- Fox, J., & Weisberg, S. (2011). *An R Companion to Applied Regression* (2nd edition). SAGE Publications, Inc.
- García Martínez, J. B., Egbejimba, J., Throup, J., Matassa, S., Pearce, J. M., & Denkenberger, D. C. (2021). Potential of microbial protein from hydrogen for preventing mass starvation in catastrophic scenarios. *Sustainable Production and Consumption*, 25, 234–247. <https://doi.org/10.1016/j.spc.2020.08.011>
- García Martínez, J. B., Pearce, J. M., Throup, J., Cates, J., Lackner, M., & Denkenberger, D. C. (2022). Methane Single Cell Protein: Potential to Secure a Global Protein Supply Against Catastrophic Food Shocks. *Frontiers in Bioengineering and Biotechnology*, 10, 906704. <https://doi.org/10.3389/fbioe.2022.906704>
- Goldin, I., & Vogel, T. (2010). Global Governance and Systemic Risk in the 21st Century: Lessons from the Financial Crisis. *Global Policy*, 1(1), 4–15. <https://doi.org/10.1111/j.1758-5899.2009.00011.x>
- Helbing, D. (2013). Globally networked risks and how to respond. *Nature*, 497(7447), Article 7447. <https://doi.org/10.1038/nature12047>
- Huang, Y., Lan, Y., Thomson, S. J., Fang, A., Hoffmann, W. C., & Lacey, R. E. (2010). Development of soft computing and applications in agricultural and biological engineering. *Computers and Electronics in Agriculture*, 71(2), 107–127. <https://doi.org/10.1016/j.compag.2010.01.001>
- IEA. (2018). *World Energy Outlook 2018*. International Energy Agency. <https://www.iea.org/reports/world-energy-outlook-2020>

- Jehn, F. U., Dingal, F. J., Mill, A., Harrison, C. S., Ilin, E., Roleda, M. Y., James, S. C., & Denkenberger, D. C. (2023). *Seaweed as a resilient food solution after a nuclear war*. Zenodo. <https://doi.org/10.5281/zenodo.7615254>
- Kassam, A., Friedrich, T., & Derpsch, R. (2019). Global spread of Conservation Agriculture. *International Journal of Environmental Studies*, 76(1), 29–51. <https://doi.org/10.1080/00207233.2018.1494927>
- Liu, H.-Y., Lauta, K., & Maas, M. (2020). Apocalypse Now?: Initial Lessons from the Covid-19 Pandemic for the Governance of Existential and Global Catastrophic Risks. *Journal of International Humanitarian Legal Studies*, 11(2), 295–310. <https://doi.org/10.1163/18781527-01102004>
- Lu, C., & Tian, H. (2016). Half-degree gridded nitrogen and phosphorus fertilizer use for global agriculture production during 1900-2013 [dataset]. In *Supplement to: Lu, C; Tian, H (2017): Global nitrogen and phosphorus fertilizer use for agriculture production in the past half century: Shifted hot spots and nutrient imbalance. Earth System Science Data, 9(1), 181-192, https://doi.org/10.5194/essd-9-181-2017*. PANGAEA. <https://doi.org/10.1594/PANGAEA.863323>
- Maggi, F., Tang, F. H. M., la Cecilia, D., & McBratney, A. (2019). PEST-CHEMGRIDS, global gridded maps of the top 20 crop-specific pesticide application rates from 2015 to 2025. *Scientific Data*, 6(1), Article 1. <https://doi.org/10.1038/s41597-019-0169-4>
- Manheim, D. (2020). The Fragile World Hypothesis: Complexity, Fragility, and Systemic Existential Risk. *Futures*, 122, 102570. <https://doi.org/10.1016/j.futures.2020.102570>
- McFadden, D. (1977). Quantitative Methods for Analyzing Travel Behaviour of Individuals: Some Recent Developments. *Cowles Foundation Discussion Papers*, Article 474.

<https://ideas.repec.org/p/cwl/cwldpp/474.html>

Mikkelsen, R. L., & Bruulsema, T. W. (2005). Fertilizer Use for Horticultural Crops in the U.S. during the 20th Century. *HortTechnology*, *15*(1), 24–30.

<https://doi.org/10.21273/HORTTECH.15.1.0024>

Moersdorf, J., Rivers, M., & Jehn, F. U. (2023). *allfed/LosingIndustryCropYields: Release for Submission* (1.1) [Computer software]. Zenodo.

<https://doi.org/10.5281/ZENODO.8198850>

Neff, R. A., Parker, C. L., Kirschenmann, F. L., Tinch, J., & Lawrence, R. S. (2011). Peak Oil, Food Systems, and Public Health. *American Journal of Public Health*, *101*(9), 1587–1597. <https://doi.org/10.2105/AJPH.2011.300123>

Neumann, K., Verburg, P. H., Stehfest, E., & Müller, C. (2010). The yield gap of global grain production: A spatial analysis. *Agricultural Systems*, *103*(5), 316–326.

<https://doi.org/10.1016/j.agsy.2010.02.004>

Ogie, R. I. (2017). Cyber Security Incidents on Critical Infrastructure and Industrial Networks.

Proceedings of the 9th International Conference on Computer and Automation Engineering, 254–258. <https://doi.org/10.1145/3057039.3057076>

Porwollik, V., Rolinski, S., Heinke, J., & Müller, C. (2019). Generating a rule-based global gridded tillage dataset. *Earth System Science Data*, *11*(2), 823–843.

<https://doi.org/10.5194/essd-11-823-2019>

Prak, M. (Ed.). (2014). *Early modern capitalism* (1st. issued in paperback). Routledge.

Rabbinge, R. (1993). The ecological background of food production. In *Crop protection and sustainable agriculture. Ciba Found. Symp. 177, John Wiley & Sons, Chicester* (pp. 2–29).

- <https://research.wur.nl/en/publications/the-ecological-background-of-food-production>
- Rawlings, J. O., Pantula, S. G., & Dickey, D. A. (1998). *Applied regression analysis: A research tool*. New York : Springer. http://archive.org/details/appliedregressio00rawl_492
- Siebert, S., Henrich, V., Frenken, K., & Burke, J. (2013). *Update of the digital global map of irrigation areas to version 5*. <https://doi.org/10.13140/2.1.2660.6728>
- Smil, V. (2017). *Energy and civilization: A history*. The MIT Press.
- Steffen, W., Richardson, K., Rockström, J., Cornell, S. E., Fetzer, I., Bennett, E. M., Biggs, R., Carpenter, S. R., de Vries, W., de Wit, C. A., Folke, C., Gerten, D., Heinke, J., Mace, G. M., Persson, L. M., Ramanathan, V., Reyers, B., & Sörlin, S. (2015). Planetary boundaries: Guiding human development on a changing planet. *Science*, 347(6223), 1259855. <https://doi.org/10.1126/science.1259855>
- Talib, M., & Mogotlhwane, T. M. (2011). Global Failure of ICT due to Solar Storm: A Worst Case Scenario Ahead. *Procedia Environmental Sciences*, 8, 371–374. <https://doi.org/10.1016/j.proenv.2011.10.058>
- Throup, J., García Martínez, J. B., Bals, B., Cates, J., Pearce, J. M., & Denkenberger, D. C. (2022). Rapid repurposing of pulp and paper mills, biorefineries, and breweries for lignocellulosic sugar production in global food catastrophes. *Food and Bioproducts Processing*, 131, 22–39. <https://doi.org/10.1016/j.fbp.2021.10.012>
- van Ittersum, M. K., Cassman, K. G., Grassini, P., Wolf, J., Tittone, P., & Hochman, Z. (2013). Yield gap analysis with local to global relevance—A review. *Field Crops Research*, 143, 4–17. <https://doi.org/10.1016/j.fcr.2012.09.009>
- Wiebe, K., Lotze-Campen, H., Sands, R., Tabeau, A., Mensbrugge, D. van der, Biewald, A., Bodirsky, B., Islam, S., Kavallari, A., Mason-D’Croz, D., Müller, C., Popp, A.,

Robertson, R., Robinson, S., Meijl, H. van, & Willenbockel, D. (2015). Climate change impacts on agriculture in 2050 under a range of plausible socioeconomic and emissions scenarios. *Environmental Research Letters*, *10*(8), 085010.

<https://doi.org/10.1088/1748-9326/10/8/085010>

Wilson, C. (2008). *High Altitude Electromagnetic Pulse (HEMP) and High Power Microwave (HPM) Devices: Threat Assessments*. Defense Technical Information Center.

Yu, Q., You, L., Wood-Sichra, U., Ru, Y., Joglekar, A. K. B., Fritz, S., Xiong, W., Lu, M., Wu, W., & Yang, P. (2020). A cultivated planet in 2010 – Part 2: The global gridded agricultural-production maps. *Earth System Science Data*, *12*(4), 3545–3572.

<https://doi.org/10.5194/essd-12-3545-2020>

Zhang, B., Tian, H., Lu, C., Dangal, S. R. S., Yang, J., & Pan, S. (2017). Global manure nitrogen production and application in cropland during 1860–2014: A 5 arcmin gridded global dataset for Earth system modeling. *Earth System Science Data*, *9*(2), 667–678.

<https://doi.org/10.5194/essd-9-667-2017>